

# Characterization of Load Sensitive Fatigue Crack Initiation in Ti-Alloys Using Crystal Plasticity Based FE Simulations

P. Chakraborty and S. Ghosh

**Abstract** Fatigue life in near  $\alpha$  Ti-alloys shows large variation with characteristics of applied load and is due to the microstructurally dependent deformation behavior in these alloys. In the present work, the load sensitive fatigue crack nucleation behavior is investigated using a physically motivated crack initiation law and cyclic crystal plasticity based finite element (CPFE) simulations of statistically equivalent image based microstructures. Since cyclic CPFE simulation for large number of cycles using conventional time integration schemes is computationally prohibitive, a wavelet transformation based multi-time scale (WATMUS) method developed in [1, 2] is used in the present work to perform accelerated simulations. To predict cycles to nucleation, a physically motivated crack nucleation model based on crystal plasticity variables developed in [3] has been used in this work. The nucleation model is calibrated and validated with experiments. The sensitivity of crack nucleation to the characteristics of the applied load is studied by performing WATMUS method based CPFE simulations for different cyclic load profiles on a statistically equivalent microstructure.

## 1 Introduction

Cycles to crack initiation in near  $\alpha$  Ti-alloys at room temperature shows large variation with characteristics of applied load. This scatter is attributed to strong influence of underlying microstructure on the deformation and fatigue behavior in these

---

P. Chakraborty (✉)  
The Ohio State University, Columbus OH-43201, USA  
e-mail: chakraborty.11@osu.edu

S. Ghosh  
Johns Hopkins University, Baltimore MD-21218, USA  
e-mail: sghosh20@jhu.edu

alloys [4–6]. A mechanistic approach is pursued in the present work to incorporate this microstructural influence on crack initiation. Similar methodology has been used in [7–12] where CPFЕ simulations of polycrystalline microstructures are performed and fatigue life models are developed based on crystal plasticity variables. Such a mechanistic approach is more accurate than conventional lifing methods where microstructural influences on fatigue life is accommodated through shifts in data curves obtained from extensive testing [13].

At room temperature, inelastic deformation in Ti-alloys predominantly happens due to slip on different slip systems in individual grains in the microstructure and is strongly size and orientation dependent. Depending on the orientation of a grain with respect to loading axis, it can have large plastic deformation (soft grain) or little or no plasticity (hard grain). Such heterogeneous plastic deformation in the polycrystalline microstructure results in stress concentration at grain interfaces and is conceived as the driver for microstructurally dependent crack nucleation in near  $\alpha$  Ti-alloys [4, 14]. A size and rate dependent CPFЕ model for near  $\alpha$  Ti-alloys developed in [15–17] captures this microstructurally dependent stress rise accurately and has been used in the present work. The morphological and crystallographical features of the polycrystalline alloys are statistically represented in the CPFЕ models [18, 19]. The use of such a statistical description not only reduces the number of grains in the FE simulations but also captures some of the key microstructural features that affect its macroscopic and microscopic responses.

Although CPFЕ simulations accurately capture the deformation behavior of polycrystalline alloys, they require very fine time steps at large applied stresses and strains when conventional time integration schemes are used. This lead to exorbitant computational requirements when fatigue analysis is performed for large number of cycles, since such reduced time steps are required in every cycle of the loading process. To resolve this computational prohibitiveness, fatigue life predictions have been performed in [7, 20, 21] by extrapolating the results based on CPFЕ simulations performed for few number of cycles. However extrapolation can lead to considerable error in the evolution of local microstructural variables and cause inaccurate fatigue life estimates based on these variables. Hence for accurate prediction, it is desirable to perform cyclic CPFЕ simulations till the failure event e.g. crack nucleation.

The dual-time behavior exhibited by the crystal plasticity variables under cyclic loading conditions allows the use of multi-time scale methods to perform accelerated FE simulations. In these methods the low and high frequency responses are decoupled and the low frequency evolution is integrated with coarser time steps to obtain computational benefit. WATMUS method developed in [1, 2] is used to perform accelerated cyclic CPFЕ simulations in the present work. This method is distinctly advantageous over other multi-time scale schemes such as the method of separation of motions [22, 23], asymptotic expansion based methods [24–26] or almost periodic temporal homogenization operator based method [27, 28] where inherent scale separation and local periodicity or almost periodicity in temporal evolution is assumed. Such assumptions are invalid for crystal plasticity variables which show strong non-periodic evolution and spatio-temporal localization. In WATMUS

method assumptions on characteristics of evolution are not made and hence proves suitable for decoupling the dual-time response of crystal plasticity variables.

A non-local crack nucleation model developed in [3] based on CPFEE variables has been used in the present work to study load dependent crack initiation in these alloys. The nucleation criterion is based on stress concentration and dislocation pile up at interface of soft and hard grains. The model is calibrated and validated with fatigue experiments performed on samples of Ti-6242. WATMUS method based cyclic CPFEE simulations of statistically equivalent image based microstructures in conjunction with the non-local crack nucleation model is used to characterize the load dependent fatigue crack initiation in near  $\alpha$  Ti-alloys. An overview of the CPFEE model and WATMUS method to perform accelerated CPFEE simulations is presented in Sects. 2 and 3 respectively. The crack nucleation model developed in [3] has been extended in the present work and is discussed in Sect. 4. A detailed numerical study of the variations in number of cycles to crack nucleation and characteristics of applied load is presented in Sect. 5.

## 2 Size and Rate Dependent CPFEE Model for Near $\alpha$ Ti-Alloys

In crystal plasticity based models, the evolution of inelastic deformation in polycrystalline alloys happens due to slip on different slip systems [29, 30]. The slip rate on the individual slip systems depend on the orientation of grains to which they belong and their resistance to slip. Hence through proper representation of orientations of grains in the underlying microstructure and slip system properties, the macroscopic and microscopic deformation behavior of polycrystalline alloys can be accurately captured through crystal plasticity based models. The morphological and crystallographical features of the microstructure are represented statistically from distributions of orientation, misorientation, size, shape of grains and microtexture, obtained from OIM scans of samples of these alloys [18, 19]. In the present work, the crystal plasticity based model and the associated parameters for near  $\alpha$  Ti-alloys reported in [15–17] has been used.

The ability of CPFEE simulations of statistically equivalent material coupon to capture microstructurally driven local event causing failure motivated the development of a crack nucleation model based on crystal plasticity variables in [3]. However fatigue life predictions using such an approach usually involve cyclic CPFEE simulations of statistically equivalent microstructures for large number of cycles. Such simulations can be computationally unachievable using conventional integration schemes. Hence WATMUS method is used to improve the efficiency of cyclic CPFEE simulations till crack nucleation and is described below.

### 3 Wavelet Transformation Based Multi-Time Scale Method for Accelerated Cyclic CPF E Simulations

Under cyclic loading, CPF E variables exhibit dual-time behavior characterized by high frequency oscillations due to applied load and low frequency monotonic response due to material relaxation that evolve with cycles. In the WATMUS method [1], decoupling of high and low frequency responses is achieved through a wavelet based transformation as shown below.

$$v^\zeta(t) = v(N, \tau) = \sum_{k=1}^n v_k(N) \psi_k(\tau) \quad \text{where } \tau \in [0, T] \quad (1a)$$

$$v_k(N) = \frac{1}{T} \int_0^T v(N, \tau) \psi_k(\tau) d\tau \quad (1b)$$

where  $v^\zeta(t)$  is single time scale variable,  $v(N, \tau)$  is the corresponding dual-scale representation,  $\psi_k(\tau)$  are wavelet basis functions that capture high frequency oscillation within each cycle,  $n$  is the number of basis functions required for accurate representation of the waveform,  $v_k(N)$  are the corresponding coefficients that evolve monotonically with cycles and  $T$  is time period of applied load. This transformation allows integration of CPF E equations in the coarse scale with time steps of cycles and provides computational benefit.

The compact support, multi-resolution and orthogonality properties of the wavelets allow significant reduction in the number of basis functions required for accurate representation of arbitrary waveforms and hence used in the method. They also eliminate spurious oscillations that arise due to considering finite number of terms from the set formed by infinitely supported basis functions like Fourier series.

In the WATMUS method, the FE weak form for quasi-static problems is transformed in terms of wavelet basis functions

$$\begin{aligned} R_{i,k}^\alpha(N) &= \frac{1}{T} \int_0^T R_i^\alpha(N, \tau) \psi_k d\tau \\ &= \sum_e \int_{V_{0,e}} \frac{1}{T} \int_0^T \frac{\partial P^\alpha}{\partial x_j} \sigma_{ji} J_e \psi_k d\tau dV_{0,e} \\ &\quad - \sum_{S_T} \int_{S_0} \frac{1}{T} \int_0^T P^\alpha t_i J_A \psi_k d\tau dS_0 = 0 \end{aligned} \quad (2)$$

where  $P^\alpha$  are the polynomial shape functions in every element  $e$ ,  $S_T$  are the surfaces on which tractions are applied,  $\alpha$  are the nodes of the discretized domain,  $V_{0,e}$  and  $S_0$  are the element volumes and surfaces in the reference configuration respectively and  $\sigma_{ji}$  are the stresses at integration points in the spatially discretized domain. The modified weak form shown in Eq. 2 is solved at discrete cyclic increments by using a Quasi-Newton scheme to obtain the wavelet coefficients of nodal displacements  $C_{i,k}^\alpha$  where

$$C_{i,k}^\alpha(N) = \frac{1}{T} \int_0^T u_i^\alpha(N, \tau) \psi_k(\tau) d\tau \quad (3)$$

and  $u_i^\alpha$  are the nodal displacement degrees of freedom of the conventional FE model. The oscillatory stress  $\sigma_{ji}(N, \tau)$  in Eq. 2 depends on the oscillatory deformation gradient  $F_{ij}(N, \tau)$  and internal variables  $y_m(N, \tau)$ .  $F_{ij}(N, \tau)$  is obtained from the coefficients of nodal displacements and the oscillatory evolution of  $y_m(N, \tau)$  in any cycle is obtained from

$$y_m(N, \tau) = y_{m0}(N) + \int_0^\tau f_m(y_m, F_{ij}, N, \tau) d\tau \quad (4)$$

where  $y_{m0}(N) = y_m(N, \tau = 0)$  are the internal variables at the start of a cycle. The initial values of internal variables  $y_{m0}$  have a monotonic evolution with cycles and form the cycle scale internal variables. Cycle scale rate equations are numerically defined for  $y_{m0}$  and is shown below.

$$\frac{\partial y_{m0}}{\partial N} = y_{m0}(N + 1) - y_{m0}(N) = y_m(N, T) - y_{m0}(N) \quad (5)$$

where

$$y_m(N, T) = y_{m0}(N) + \int_0^T f_m(y_m, F_{ij}, N, \tau) d\tau \quad (6)$$

Since  $f_m$  are non-linear functions, numerical integration using backward Euler scheme is used in Eq. 6. The cycle scale internal variables are integrated using second order backward difference formula as shown below.

$$y_{m0}(N) = \beta_1 y_{m0}(N - \Delta N) - \beta_2 y_{m0}(N - \Delta N - \Delta N_p) + \beta_3 \left. \frac{\partial y_{m0}}{\partial N} \right|_N \Delta N$$

where  $\beta_1 = \frac{(r+1)^2}{(r+1)^2 - 1}$   $\beta_2 = \frac{1}{(r+1)^2 - 1}$   $\beta_3 = \frac{(r+1)^2 - (r+1)}{(r+1)^2 - 1}$

and  $r = \frac{\Delta N_p}{\Delta N}$  (7)

A Newton-Raphson scheme is used to integrate Eq. 7.

To reduce the number of global degrees of freedom, only the evolving wavelet coefficients of nodal displacements are solved at any cyclic increment from the cycle scale weak form shown in Eq. 2. These coefficients are selected based on criterion developed in [1]. The evolution of CPFE variables saturates with advancing load and integration of the coarse variables can be performed with larger cycle jumps. Hence, prediction of cycle jumps are made based on an upper bound on the error in truncation of Taylor series in second order backward difference formula in Eq. 7. The use of these adaptive criteria significantly enhances the performance of WATMUS method to perform cyclic CPFE simulations.

## 4 Non-Local Crack Initiation Model for Near $\alpha$ Ti-Alloys

In the present work, fatigue crack nucleation studies are made using the model developed in [3]. The model is motivated from experimental observations of failed Ti-6242 samples under fatigue loading with maximum stress at 90–95 % of yield strength and stress ratio  $\sigma_{min}/\sigma_{max} = 0$ . Detailed experimental investigations performed at failure sites suggest that regions with hard grains surrounded by soft grains are susceptible to initiate sub-surface cracks in near  $\alpha$  Ti-alloys [31, 32].

In the presence of soft grains with large plastic deformation adjacent to hard grains, large stresses develop in the hard grains to satisfy strain compatibility condition. Additionally, dislocation motions causing plastic deformation in soft grains are prevented at hard-soft grain interfaces which results in piling up of these dislocations at the interface. In the crack nucleation model both these aspects are considered. It is hypothesized that the pile up of dislocation at the interface cause micro crack formation in hard grains. These micro cracks experience large stresses in hard grains and propagate to form macroscopic crack nucleation sites. A stress intensity factor  $R$  is defined for the growth of micro cracks as shown below

$$R = T_{eff}\sqrt{c} \quad \text{and} \quad T_{eff} = \sqrt{\langle T_n \rangle^2 + \beta T_t^2} \quad (8)$$

where  $c$  is the micro-crack length and  $T_{eff}$  is the effective traction on crack plane. Both shear  $T_t$  and normal  $T_n$  component of traction are considered. Since compressive nature of normal traction  $T_n$  cause crack closure, a Macaulay bracket is used implying compressive normal traction has no effect on the stress intensity factor  $R$ .

The micro crack length  $c$  is related to dislocation pile up length  $B$  in adjacent soft grain using the relation proposed in [33]. In the formula, the equilibrated wedge shaped micro-crack length  $c$  is given by

$$c = \frac{G}{8\pi(1-\nu)\gamma_s} B^2 \quad (9)$$

where  $G$  is the shear modulus and  $\gamma_s$  is the surface energy. The dislocation pile length  $\mathbf{B}$  is evaluated from closure failure around any burgers circuit due to inhomogeneous plastic deformation as shown below

$$\mathbf{B} = \oint_{\Gamma} d\bar{\mathbf{x}} = \oint_{\Gamma} \mathbf{F}^p d\mathbf{X} = \int_{\Omega} \mathbf{A} \cdot \mathbf{n} d\Omega \quad (10)$$

where  $\mathbf{n}$  is normal to surface  $\Omega$  in which the burger's circuit is considered and  $\mathbf{A}$  is Nye's dislocation tensor which depends on curl of  $\mathbf{F}^p$

$$\mathbf{A} = \nabla^T \times \mathbf{F}^p \quad (11)$$

The stress intensity factor  $R$  evolves with increasing cycles of applied load. Macroscopic crack nucleation is considered to happen when  $R$  at any material point on the interfaces of hard soft grains in the microstructure exceeds the critical stress intensity factor  $R_c$ . The critical stress intensity factor  $R_c$  is a material constant for a given alloy and is calibrated from experiments.

In the present work, load sensitive fatigue life of Ti-6242 is investigated. Hence,  $R_c$  is evaluated for this alloy from WATMUS based cyclic CPFE simulations and dwell fatigue experiments. A detailed description of the calibration procedure is provided in [3]. The procedure is extended in the present work by considering the basal plane as the plane of crack nucleation to determine  $R$ . Using in situ surface acoustic wave techniques and dwell fatigue experiments performed on different samples of Ti-6242, it has been observed that crack initiation happens at 80–85 % of total number of cycles to failure [34]. Based on this observation, a lower and upper bound on  $R_c$  is determined and these are

$$\begin{aligned} \text{Crack nucleation at 80 \% of total life} \quad R_{c(80\%)} &= 6.54 \text{ MPa}\sqrt{\mu\text{m}} \\ \text{Crack nucleation at 85 \% of total life} \quad R_{c(85\%)} &= 6.80 \text{ MPa}\sqrt{\mu\text{m}} \end{aligned}$$

## 5 Sensitivity of Cycles to Crack Nucleation to Characteristics of Applied Load

A statistically equivalent microstructure of Ti-6242 is considered to correlate cycles to crack nucleation and characteristics of applied load. Two separate studies has been performed. In the first study, comparisons between dwell load, normal cyclic load and maximum stress levels are performed. In the second study, the effect of hold-time in the dwell load on cycles to crack nucleation has been studied.

### 5.1 Comparison Between Dwell and Normal Cyclic Load

In this sensitivity study the statistically equivalent microstructure is subjected to 4 different types of load as shown below:

- Case A:  $\sigma_{max} = 894$  MPa,  $\sigma_r = 0$ ,  $T_{load} = T_{unload} = 1$  s and  $T_{hold} = 120$  s
- Case B:  $\sigma_{max} = 847$  MPa,  $\sigma_r = 0$ ,  $T_{load} = T_{unload} = 1$  s and  $T_{hold} = 120$  s
- Case C:  $\sigma_{max} = 894$  MPa,  $\sigma_r = 0$ ,  $T_{load} = T_{unload} = 61$  s and  $T_{hold} = 0$  s
- Case D:  $\sigma_{max} = 894$  MPa,  $\sigma_r = 0$ ,  $T_{load} = T_{unload} = 1$  s and  $T_{hold} = 0$  s

Maximum applied stress ( $\sigma_{max}$ ) is 95 % of yield strength in cases A, C and D and is 90 % of the yield strength in case B. Dwell load with 2 min hold is applied in cases A and B. Triangular load with time periods  $T = 122$  and  $T = 2$  s is applied in cases C and D respectively. WATMUS method is used to perform cyclic CPFÉ simulations and stress intensity factor  $R$  is evaluated at nodes situated at grain interfaces. In a cycle,  $R$  is evaluated at start of unloading and corresponds to  $\tau = 121$  s in cases A and B,  $\tau = 61$  s in case C and  $\tau = 1$  s in case D. The evolution  $R$  at the node where crack nucleation is predicted using calibrated  $R_c$  is shown in Fig. 1.

The number of cycles to crack initiation based on calibrated  $R_c$  values at 80 and 85 % of total life is summarized in Table 1. As can be observed from the table, the microstructure has a shorter fatigue initiation life when subjected to dwell load (cases A and B) as compared to normal cyclic loading (cases C and D). The number of cycles to crack nucleation for dwell (case A) and normal fatigue (case D) at 95 % of yield strength shows the same trend as observed experimentally [4–6]. In the normal cyclic loading cases, the decrease in frequency of the load deteriorates the life of the microstructure as can be observed from cases C and D. Also it can be observed from this study that an increased maximum stress in normal cyclic loading (cases C and

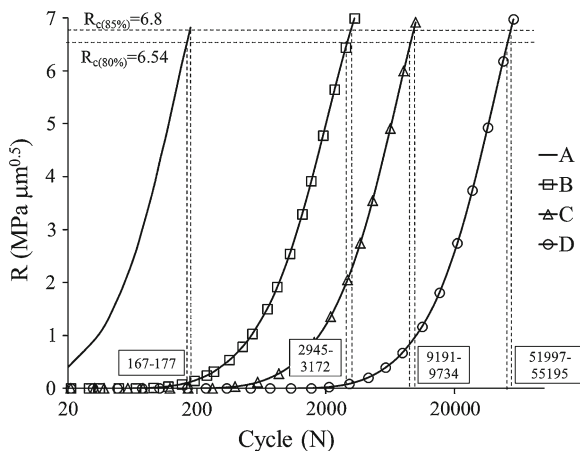


**Fig. 1** Evolution of  $R$  with cycles at the predicted crack initiation site for 4 different fatigue load cases A,B,C and D



**Table 1** Comparison of number of cycles to crack initiation for different cyclic load forms

Case No.	Cycles to crack nucleation	
	80 % of life	85 % of life
A	167	177
B	2945	3172
C	9191	9734
D	51997	55195

D) is less detrimental than the hold at a lower maximum stress under dwell loading (case B).

### 5.2 Comparison Between Different Hold Times for Dwell Load

The number of cycles to crack nucleation for different hold time and same time period of dwell with maximum applied stress at 95 % of yield strength, is also compared for this statistically equivalent microstructure. WATMUS based CPFE simulations are performed for three different load cases shown below:

- Case E:  $T_{load} = T_{unload} = 16$  s and  $T_{hold} = 90$  s
- Case F:  $T_{load} = T_{unload} = 31$  s and  $T_{hold} = 60$  s
- Case G:  $T_{load} = T_{unload} = 46$  s and  $T_{hold} = 30$  s

The number of cycles to initiate a crack is evaluated from non-local crack nucleation model described in Sect. 4. The evolution of  $R$  at the crack initiation site is

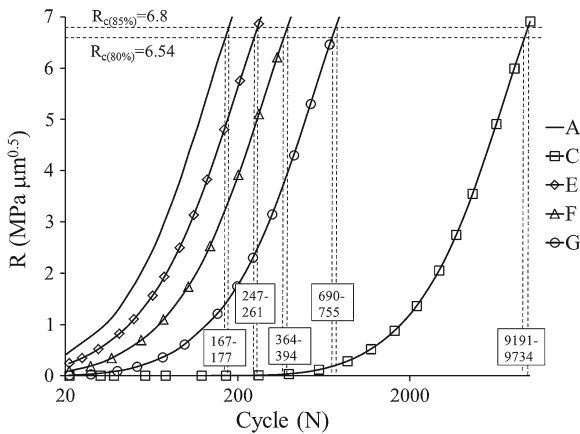
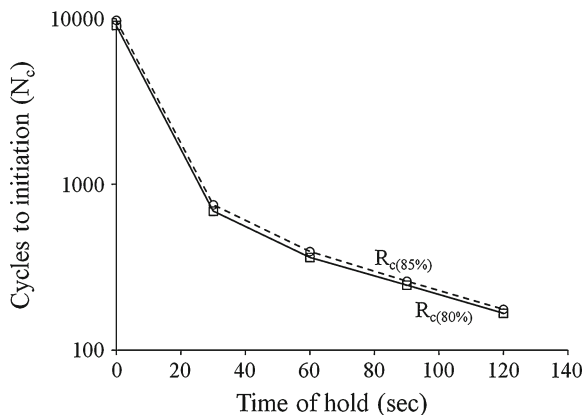


**Fig. 2** Evolution of  $R$  with Cycles for 5 different fatigue load cases A,E,F,G and C

**Fig. 3** Comparison of number of cycles to crack initiation for different hold time at maximum stress



shown in Fig. 2. A plot of number of cycles to crack initiation versus hold time is shown in Fig. 3. A definite trend in life to initiation with hold time can be observed.

## 6 Conclusion

Fatigue crack nucleation in near  $\alpha$  Ti-alloys is strongly influenced by its underlying microstructure and a mechanistic approach based on CPFE simulations of statistically equivalent microstructures in conjunction with a physically motivated crack nucleation model is pursued in the present work to accurately predict this behavior. WATMUS method is used to perform accelerated cyclic CPFE simulations which is otherwise infeasible. A non-local crack nucleation model based on micro-crack growth under the influence of local stresses at hard soft grain interfaces is used to predict initiation. A critical stress intensity factor is defined that dictates crack nucleation and is calibrated from dwell fatigue experiments performed on samples of Ti-6242. A statistically equivalent microstructure is subjected to different cyclic load patterns and cycles to crack nucleation is predicted from the proposed model. From the predictions, a trend in cycles to crack initiation and hold, loading, unloading time and maximum applied stress level can be observed.

In the present work the workability of the proposed integrated computational and experimental approach to quantify scatter in fatigue crack nucleation in near  $\alpha$  Ti-alloys has been demonstrated. The methodology can be extended to other polycrystalline alloy systems for accurate fatigue life predictions and is considered as a future work.

## References

1. Joseph, D.S., Chakraborty, P., Ghosh, S.: *Comp. Methods. App. Mech. Engg.* **199**, 2177 (2010)
2. Chakraborty, P., Joseph, D.S., Ghosh, S.: *Finite Elem. Ana. Des.* **47**, 610 (2011)
3. Anahid, M., Samal, M.K., Ghosh, S.: *J. Mech. Phys. Solids* **59**(10), 2157 (2011)
4. Bache, M.R.: *Int. J. Fatigue* **25**, 1079 (2003)
5. Bache, M.R., Cope, M., Davies, H.M., Evans, E.J., Harrison, G.: *Int. J. Fatigue* **19**(93), 83 (1997)
6. Sinha, V., Mills, M.J., Williams, J.C.: *Metall. Mat. Trans. A* **35**, 3141 (2004)
7. Sinha, S., Ghosh, S.: *Int. J. Fatigue* **28**, 1690 (2006)
8. Goh, C.H., Wallace, J.M., Neu, R.W., McDowell, D.L.: *Int. J. Fatigue* **23**, 5423 (2001)
9. Sackett, E., Germain, L., Bache, M.: *Int. J. Fatigue* **29**, 2015 (2007)
10. Bridiera, F., McDowell, D.L., Villechaisea, P., Mendez, J.: *Int. J. Plasticity* **25**, 1066 (2009)
11. Mineur, M., Villechaise, P., Mendez J.: *Mater. Sci. Engg. A* **286**, 257—268 (2000)
12. McDowell, D., Dunne, F.P.E.: *Int. J. Fatigue* **32**, 1521 (2010)
13. Suresh, S.: *Fatigue of Materials*. Cambridge University Press, Cambridge (1998)
14. Lutjering, G., Williams, J.C.: *Titanium*. Springer-Verlag, Berlin-Heidelberg (2007)
15. Hasija, V., Ghosh, S., Mills, M.J., Joseph, D.S.: *Acta Mater.* **51**, 4533 (2003)
16. Deka, D., Joseph, D.S., Ghosh, S., Mills, M.J.: *Metall. Trans. A.* **37**(5), 1371 (2006)
17. Venkatramani, G., Ghosh, S., Mills, M.J.: *Acta Mater.* **55**, 3971 (2007)
18. Groeber, M., Ghosh, S., Uchic, M.D., Dimiduk, D.M.: *Acta. Mat.* **56**, 1257 (2008)
19. Groeber, M., Ghosh, S., Uchic, M.D., Dimiduk, D.M.: *Acta. Mat.* **56**, 1274 (2008)
20. Bennett, V.P., McDowell, D.L.: *Int. J. Fatigue* **25**, 27 (2003)
21. Turkmen, H.S., Loge, R.E., Dawson, P.R., Miller, M.: *Int. J. Fatigue* **25**, 267 (2003)
22. Blekhman I.I.: *Vibrational mechanics*. World Scientific, Singapore (2000)
23. Thomsen, J.J.: *Vibrations and stability: theory, analysis and tools*, 2nd edn. Springer-Verlag, Berlin (2004)
24. Yu, Q., Fish, J.: *Comput. Mech.* **29**, 199 (2002)
25. Manchiraju, S., Asai, M., Ghosh, S., Strain Anal, J.: *Engg. Des.* **42**, 183 (2007)
26. Manchiraju, S., Kirane, K., Ghosh, S.: *J. Comp. Aid. Mater. Des.* **14**, 47 (2008)
27. Oskay, C., Fish, J.: *Int. J. Multiscale. Comput. Engg.* **2**, 1 (2004)
28. Oskay, C., Fish, J.: *Int. J. Num. Methods Engg.* **61**, 329 (2004)
29. Anand, L., Kothari, M.: *J. Mech. Phys. Solids* **44**(4), 525 (1996)
30. Kalidindi, S.R., Bronkhorst, C.A., Anand, L.: *J. Mech. Phys. Solids* **40**, 537 (1992)
31. Sinha, V., Spowart, J.E., Mills, M.J., Williams, J.C.: *Metall. Mat. Trans. A* **37**, 1507 (2006)
32. Sinha, V., Mills, M.J., Williams, J.C.: *Metall. Mat. Trans. A* **37**, 2015 (2006)
33. Stroh, A.N.: *Proc. R. Soc. Lond. Ser. A* **223**, 404 (1954)
34. Rokhlin, S., Kim, J.Y., Zoofan, B.: unpublished research. The Ohio State University, Columbus (2005)